

# Muon $g-2$ Anomaly in the Mirror Twin Higgs Models

Guo-Li Liu<sup>1\*</sup>, Ping Zhou<sup>2,3,4†</sup>

<sup>1</sup>*School of Physics and Microelectronics,*

*Zhengzhou University, Zhengzhou 450001, Henan, China*

<sup>2</sup>*National Space Science Center, Chinese Academy of Sciences, Beijing 100190, China*

<sup>3</sup>*University of Chinese Academy of Sciences, Beijing 100140, China*

<sup>4</sup>*Beijing Key Lab of Space Environment Exploration, Beijing 100140, China*

## Abstract

We examine the muon  $g - 2$  anomaly of the mirror twin Higgs models with the joint constraints of the Higgs global fit data, the precision electroweak data, the leptonic flavor changing decay  $\mu \rightarrow e\gamma$  decays, and the mass requirement of the heavy gauge bosons. It is concluded that the muon  $g-2$  anomaly is very sensitive to two parameters:  $0.03 \leq y_{\nu l} \leq 0.09$  and  $0.4 \leq y_t \leq 0.8$ , while other parameters are almost irrelevant.

PACS numbers: 12.60.-i, 12.60.Fr

---

\* Email address: guoliliu@zzu.edu.cn

† Email address: pzhou@nssc.ac.cn

## I. INTRODUCTION

Since the announcement was made by the E821 experiment in 2001 [1], the muon anomalous magnetic moment  $g - 2$  has been a long-standing puzzle. As a very precisely measured observable, it is expected to shed light on "new physics". The current world-averaged result[2] of the precision measurement of  $a_\mu = (g - 2)/2$ , which has been performed by the E821 experiment at Brookhaven National Laboratory [3], is given by

$$a_\mu^{exp} = 116592091(\pm 54)(\pm 33) \times 10^{-11}, \quad (1)$$

and the discrepancy with the standard model (SM) prediction [4] is  $3.7\sigma$ ,

$$\Delta a_\mu = a_\mu^{exp} - a_\mu^{SM} = (281 \pm 76) \times 10^{-11}. \quad (2)$$

It may hint the existing of the new physics beyond the SM. The difference between the experimental data and the SM prediction determines there is room for the possible new physics to live in.

Various new physics scenarios try to explain the muon  $g - 2$  excess, for recent reviews, see e.g. Refs. [5–9]. Among these new physics models, the left-right twin Higgs model may also accommodate the possibilities for the muon  $g - 2$  anomaly[10], in which the extra scalars can give positive contributions to muon  $g - 2$  via the two-loop Barr-Zee diagrams.

The so called mirror twin Higgs (MTH) models can be realized by extending the SM with the mirror symmetry[11], and in these models, via the extending group, we have the flavor changing couplings of the leptons and the quarks through the charged extra gauge bosons and the scalars[12–14], which will contribute to the two-loop Barr-Zee diagrams of the muon anomaly magnetic moment.

From Ref.[14], we can see that the one-loop contributions to the muon anomalous magnetic moment are too small, about  $10^{-11}$  for  $m_\nu = 10$  TeV, and it is too small to remedy the discrepancy between the experiments and the theoretical calculation in Eq.(2). That is to say, it is far beyond the scope of the detectable level, as long as the heavy neutrino mass is not too far great. So we will in the following turn to the two-loop level contribution.

As we know, in some case, since the quarks are much heavier than the leptons, the phase space depression may be surpassed by the mass enhancement, so the two-loop Barr-Zee diagrams may contribute much more largely than that from the one-loop ones, if the Higgs bosons are not too light[15, 16].

In this work we will examine the parameter space of MTH by considering the joint fits from the theory, the precision electroweak data, the 125 GeV Higgs signal data, the muon  $g - 2$  anomaly, the lepton rare decay of  $\mu \rightarrow e\gamma$ , as well as the direct search limits from the LHC.

This work is organized as follows. In Sec. II we recapitulate the effective couplings of the MTH model. In Sec. III the two-loop muon  $g - 2$  anomaly and other relevant constraints are discussed. In Sec. IV, we will use the direct search limits from the LHC, especially the Higgs global fit to constrain the model parameters. Finally, Sec. VI gives the conclusion.

## II. THE MTH MODELS AND THE RELEVANT COUPLINGS

### A. The models with a mirror symmetry–mirror twin Higgs models

The hierarchy problem [17–19], which is induced by the disparity between the electroweak scale and the Planck scale, is one of the most outstanding problems in particle physics (see, e.g., [20]). Both supersymmetry [21] and the compositeness of the Higgs [22], even the strong breaking models [23], where the electroweak scale originates from a supersymmetry breaking scale or a composite scale, or even abandoning the idea of the Higgs as the origin of the electroweak symmetry breaking, have attempted to address the issue. Without the fine-tuning parameters, however, these classes of solutions in the new physics models mentioned above generically contain the top quark partners which have SM colored charge with the mass at the electroweak scale. Such particles have very rich phenomenological possibilities which are easily found at the Large Hadron Collider (LHC), while, so far, there is not any signal of this kind of particles, which constrains their masses severely: typically larger than 1 TeV [24, 25]. To satisfy the bounds of this kind, the parameters in these theories need to be fine-tuned to fix the electroweak scale. This fine-tuning is called the little hierarchy problem.

One solution to the little hierarchy problem is to assume that the Higgs mass is protected by a discrete symmetry, so the new particles associated with this symmetry do not have the SM color charge. This situation makes the new particle states much more difficult to be produced and detected at the large hadron colliders.

To stabilize the Higgs mass up to scales of order 5 – 10 TeV, a lot of theories of this

kind [11, 26–34], have been proposed. The MTH [11] model is one of the best known examples, in which the symmetry mechanism avoids the little hierarchy via introducing a  $Z_2$  symmetry that copies the SM particles and introduces an approximate global symmetry of the Higgs potential. After the twin Higgs obtains a vacuum expectation value  $f$ , the SM Higgs has become into a pseudo-Nambu-Goldstone (pNG) boson, preventing the Higgs mass from quantum corrections up to the scale  $\Lambda_{TH} \sim 4\pi f$  because of the mirror symmetry between the top and the top partner. Now, the top quark partner is not SM colored, but twin colored, so does not have rich phenomenologies and is not easily produced and probed at the LHC, thereby the little hierarchy problem settled down.

Since it has been discussed in the left-right twin Higgs models[10], the reason that we reconsider the  $g - 2$  in this model is as follow. After realizing the natural electroweak breaking, the pNG mass is at most logarithmically divergent. Thus corrections to precision electroweak observables can be naturally small, which provides a resolution to the LEP paradox. The MTH models are quite appealing, since, firstly, the discrete mirror symmetry in them corresponds the extended fields with the SM ones. Secondly, the extended fields are uncharged under the SM gauge groups, that is to say, they will appear as singlets, and "show" in upcoming experiments purely as missing energy, escaping from the current constraints of the LHC to the new particles. The left-right symmetric models [35] with lighter gauge bosons and the vector-like fermions, however, lead to rich detectable phenomenology for upcoming experiments, and are in challenge with nowadays stringent experimental constraints.

### **B. The general form of the flavor changing couplings among leptons and quarks in the MTH models [12, 13]**

Since the minimal coset  $U(4)/U(3)$  does not contain a residual custodial symmetry, and in the non-linear case the twin mechanism is not realized in the gauge sector within this global group, while  $SO(8)/SO(7)$  prevents a large custodial breaking in composite models of the twin mechanism, the global symmetry breaking pattern of the simplest MTH model can be  $SO(8)/SO(7)$  case[12, 13, 36, 37]. The 7 pNGBs after the breaking are encoded in the field  $U$  obtained by the exponentiation of the fluctuations associated with the broken generators,

$$U = \exp i \frac{\Pi}{f}. \quad (3)$$

Defining the pNGB matrix  $\Pi$  containing the 7 goldstones as

$$\Pi = \sqrt{2}\pi^{\hat{a}}T^{\hat{a}}, \quad \hat{a} = 1, \dots, 7, \quad (4)$$

where  $T^{\hat{a}}$  are the broken generators, defined as

$$T_{ij}^{\hat{a}} = -\frac{i}{\sqrt{2}}t_{ij}^{\hat{a}8}, \quad \hat{a} = 1, \dots, 7. \quad (5)$$

here  $t_{ij}^{ab} = \delta_i^a\delta_j^b - \delta_j^a\delta_i^b$ , and  $\pi^{\hat{a}}$  are the goldstone fields in the  $\mathbf{7}$  of  $\text{SO}(7)$ .

Giving  $\Sigma_i \equiv U_i^8$ ,

$$\Sigma = U(\pi)\Sigma_0 = \left( \pi_1 \ \pi_2 \ \pi_3 \ \pi_4 \ \pi_5 \ \pi_6 \ \pi_7 \ \sigma \right)^T, \quad \sigma = \sqrt{1 - \pi_a^2}, \quad (6)$$

But, actually, these are not the only global symmetries, and to realize the twin Higgs mechanism we have to include a mirror copy of QCD, which means having an unbroken  $\text{SU}(3)_c \times \text{SU}(3)'_c \times Z_2$ . So the global symmetry is actually

$$\frac{G}{H} = \frac{\text{SU}(3)_c \times \text{SU}(3)'_c \times Z_2 \times \text{SO}(8)}{\text{SU}(3)_c \times \text{SU}(3)'_c \times Z_2 \times \text{SO}(7)}. \quad (7)$$

We parameterize the Higgs and its twin via the decomposition  $\mathbf{8} = (\mathbf{2}, \mathbf{1}, \mathbf{2}) + (\mathbf{1}, \mathbf{2}, \mathbf{2})$  under  $\text{SU}(2)_L \times \text{SU}(2)_{\tilde{L}} \times \text{SU}(2)_{\tilde{R}}$  as

$$(\mathbf{2}, \mathbf{1}, \mathbf{2}) : H = \frac{f}{\sqrt{2}} \begin{pmatrix} \pi_2 + i\pi_1 \\ h - i\pi_3 \end{pmatrix}, \quad (\mathbf{1}, \mathbf{2}, \mathbf{2}) : \tilde{H} = \frac{f}{\sqrt{2}} \begin{pmatrix} \pi_6 + i\pi_5 \\ \sigma - i\pi_7 \end{pmatrix}, \quad (8)$$

where  $\pi_2 + i\pi_1$  can be identified as the charged scalar, and  $\tilde{\omega}^{\pm} \equiv f(\pi_6 \pm i\pi_5)/\sqrt{2}$  and  $\tilde{\omega}_0 \equiv f\pi_7$  are eaten by the gauge bosons. Here  $h \equiv \pi_4$ .

The SM gauge fields acquire the typical masses proportional to the scale of electroweak symmetry breaking,  $v$ . The mirror gauge fields, on the other hand, are not inside of  $\text{SO}(7)$  and acquire masses proportional to the goldstone scale,  $f$ , instead.

At low energies the interactions of  $q_L$  and  $\tilde{q}_L$  can be simply obtained

$$\begin{aligned} Q_L = v_b b_L + v_t t_L &= \frac{1}{\sqrt{2}} \begin{pmatrix} i b_L & b_L & i t_L & -t_L & 0 & 0 & 0 & 0 \end{pmatrix}^T, \\ \tilde{Q}_L = \tilde{v}_b \tilde{b}_L + \tilde{v}_t \tilde{t}_L &= \frac{1}{\sqrt{2}} \begin{pmatrix} 0 & 0 & 0 & 0 & i \tilde{b}_L & \tilde{b}_L & i \tilde{t}_L & -\tilde{t}_L \end{pmatrix}^T, \end{aligned} \quad (9)$$

while those of  $t_R$  and  $\tilde{t}_R$  are  $\text{SO}(7)$  singlets. Thus the top Yukawa couplings are written as

$$y_t f \bar{t}_R \Sigma^\dagger Q_L + \tilde{y}_t \tilde{f} \tilde{t}_R \Sigma^\dagger \tilde{Q}_L + \text{h.c.} = -y_t \bar{q}_L H t_R - \tilde{y}_t \tilde{t}_R \tilde{H} \tilde{q}_L + \text{h.c.}, \quad (10)$$

where  $q_L = (b, t)$ ,  $\tilde{q}_L = (\tilde{b}, \tilde{t})$ .

A  $Z_2$  symmetry  $q_L, t_R \leftrightarrow \tilde{q}_L, \tilde{t}_R$  leads to  $y_t = \tilde{y}_t$ . The masses of the rest fermions (including twin fermions) are obtained in a similar manner. Due to  $\tilde{y}_\psi \ll y_t$  the associated contribution to the Higgs potential of the light fermions will be negligible, so it is not needed to enforce the approximate equality  $y_\psi = \tilde{y}_\psi$ .

From the above discussion, we can see that the mediated particles which induce the lepton flavor violating(LFV) couplings could be bosons or scalars, in addition to the massive right-handed neutrinos. We summarize in the following the general forms of the LFV couplings from the effective Lagrangian of leptonic sector[38, 39],

$$\begin{aligned} \mathcal{L} = & V_{ji}U_{\ell_j i}^* \bar{\nu}_i W_\mu^+ \gamma^\mu P_L \ell_j + y_{ji}U_{\ell_j i}^* \bar{\nu}_i H^+ P_R \ell_j + h.c. \\ & + \lambda_\ell \bar{\ell} H^0 \ell + g_\ell \bar{\ell} Z_\mu^0 \gamma^\mu P_L \ell + \lambda_{ji} \bar{\ell}_i H^0 \ell_j + g_{ji} \bar{\ell}_i Z_\mu^0 \gamma^\mu (f_v + f_a \gamma^5) \ell_j + h.c., \end{aligned} \quad (11)$$

$g_\ell$ ,  $\lambda_\ell$  is the coupling of the heavy neutral boson and the scalar to the charged lepton, and  $g_{ji}$ ,  $\lambda_{ji}$  is the couplings between the leptons of different flavors. We consider the vector- ( $f_v$ ) and the axis-form ( $f_a$ ) structure of the couplings to the different flavors.

In the following calculation, we assume that the right-handed neutrinos are degenerate, i.e,  $m_1 = m_2 = m_3 = m_\nu$ , which means that there is only one flavor of the heavy neutrino, so the couplings  $V_{ji}$  and  $y_{ji}$  will be simply written as  $V_j$  and  $y_j$ , respectively.

Note that there should be a  $3 \times 3$  Maki-Nakagawa-Sakata (MNS) matrix  $U_{MNS}$  [40, 41] in the flavor changing couplings, however, we here absorb all this matrix into the couplings and take them as free parameters.

### III. MUON ANOMALOUS MAGNETIC MOMENT $g - 2$ AND THE RELEVANT CONSTRAINTS

#### A. Numerical calculations

In this paper, we take the light CP-even Higgs  $h$  as the SM-like Higgs,  $m_h = 125.5$  GeV. Since the muon  $g - 2$  anomaly favors a small charged pseudoscalar mass and large Yukawa couplings, we will scan over  $m_H$  in the following ranges:

$$100 \text{ GeV} < m_{H^\pm} < 1000 \text{ GeV}. \quad (12)$$

In the following, we will give the constraints on the parameters:

- (1) The first constraint come from the signal data of the 125 GeV Higgs, which is important, since the couplings of the SM-like Higgs with the fermions and the bosons in MTH models can deviate from the SM largely and the production and decay modes of the SM-like Higgs may be modified severely. In the paper, we will perform the calculation of  $\chi_h^2$  for the signal strengths of the 125.5 GeV Higgs, which will be given detailedly in Sec. IV.
- (2) The joint effects from the  $Z$ -pole precision measurements, the low energy neutral current process and the high energy precision measurements off the  $Z$ -pole indirectly constraint the  $f$  parameter, which is preferred to be larger than 500-600 GeV according to all these data[42]. On the other hand, to control in mild fine tuning,  $f$  should not be too large since the fine tuning is more severe for large  $f$ .

Constraints for  $f$  from the flavor changing decay  $\mu \rightarrow e\gamma$ : With the experimental constraints Refs[43],  $BR(\mu \rightarrow e\gamma) < 4.2 \times 10^{-13}$ , the flavor changing decay  $\mu \rightarrow e\gamma$  will give  $f \sim [0.6 - 2]$  TeV.

So after we take the above constraints from the electroweak precision measurements and the LHC data into account, we can assume that  $500GeV \leq f \leq 2000GeV$ .

In our numerical evaluations, however, we have not taken  $f$  as free parameter. Instead, we assume the characteristic mass and coupling of the composite resonances is set by  $m$  and  $g$  respectively, which are related by the symmetry-breaking order parameter,  $f$ , as  $m = gf$ .

- (3) In the nowadays experiments,  $m_{W_H^\pm}$  has been constrained stringently [44–46]. The ATLAS experiment has presented the first search for dilepton resonances based on the full Run 2 data set [44, 46] and set limits on the  $W'$  production cross sections times branching fraction in the process

$$\sigma(pp \rightarrow W'X) \times BR(W' \rightarrow \nu\ell) \tag{13}$$

for  $M'_W$  in the 0.15 TeV – 7 TeV range, correspondingly. Recently, similar searches have also been presented by the CMS Collaboration using 140  $fb^{-1}$  of data recorded at  $\sqrt{s} = 13$  TeV [45]. The most stringent limits on the mass of  $W'$  boson to date come from the searches in the above process by the ATLAS and CMS collaborations using

data taken at  $\sqrt{s} = 13$  TeV in Run 2 and set a 95% confidence level (CL) lower limit on the  $W'$  mass of 6.0 TeV [46].

This analysis, however, is based on the simplest models[47] such as the sequential standard model proposed by Altarelli et al.,[48], which is usually taken as a convenient benchmark in the experiments. In the simplest models the gauge particles are considered copies of the SM gauge bosons, and they couple to fermions, which is in the same mode as those of the SM gauge bosons, but miss trilinear couplings such as  $W'WZ$  and  $Z'WW$ , etc. So the situation that the sequential standard model[48] has acted as a reference for experimental extended gauge boson searches may be changed and the results may be re-interpreted in the context of other new physics models [49]. We in the computation will try the mass in the range  $1 \leq m_{W_{\pm}^{\pm}} \leq 20$  TeV to check the sensitivity of the charged heavy gauge boson mass.

- (4) About the top Yukawa  $y_t$ , since in general, we assume that the top quark is connected to electroweak symmetry breaking and sensitive to the new physics models, we scan it from zero to 1.5 times of the SM top Yukawa  $y_t^{SM}$ . The same is the heavy gauge boson couplings to the lepton  $y_{\nu W}$ , also from zero to 1.5 times of the SM couplings  $y_{\nu W}^{SM}$ . As for the charged Higgs couplings to the lepton,  $y_{\nu \ell}$ , which is absent in the SM in the unitary gauge, we choose it in the range:  $0 \leq y_{\nu \ell} \leq 0.1$ .

## B. Two-Loop Barr-Zee Muon $g - 2$ in the MTH models

In the MTH, the two-loop Barr-Zee muon  $g - 2$  contributions are mediated by the charged Higgs  $H^{\pm}$  and the extra gauge boson  $W_{H}^{\pm}$ . With the large quark mass, the quite large enhancement factor  $m_q^2/m_{\mu}^2$  surpass the loop suppression phase space factor  $\alpha/\pi$ , so the two-loop contributions could be more important than one-loop ones. Moreover, we note that in the Barr-Zee two-loop diagrams there are no two scalars or two  $W^{\pm}$  charged bosons connect to the triangle loop simultaneously due to the helicity constraints. Since between the two charged particles in the quark loop, the fermion is the bottom quark, the slash momentum terms must vanish undergoing a single  $\gamma$  matrix because of the much smaller mass of the bottom quark compared to the top quark, shown as Fig.1(b). Thus, the only contribution comes from Fig.1(a). In Fig.1, there is no contribution from the twin charged

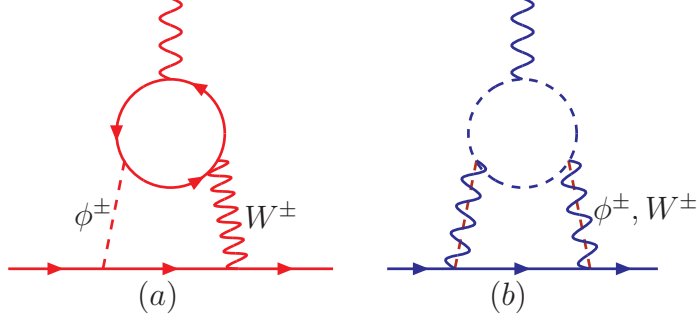


FIG. 1: The potential two-loop contributions to  $a_\mu$  the MTH models.

Higgs, since in Eq.(8), we can see that the charged parts are absorbed into the charged bosons and don't exist actually. The fermion loop, however, can consist of not only top and bottom quark  $t\bar{t}b$ ,  $b\bar{b}t$ , but also the lepton with the right-handed neutrino  $\ell\nu_R$ , since the neutrino mass might be quite large.

The Barr-Zee two-loop contribution can be written as[10, 50–53],

$$\begin{aligned} \Delta a_\mu(t\bar{t}b + b\bar{b}t) = & -\frac{4m_\mu^2}{e} \frac{-e^3}{1024\pi^4 \sin^2\theta_w} \frac{N_t^c V_{tb}^*}{m_{H^+}^2 - m_W^2} \\ & \int_0^1 dx [Q_t x + Q_b(1-x)] \left[ G\left(\frac{m_t^2}{m_{H^+}^2}, \frac{m_b^2}{m_{H^+}^2}\right) - G\left(\frac{m_t^2}{m_W^2}, \frac{m_b^2}{m_W^2}\right) \right] \\ & \times \left[ \left( \Gamma_{tb}^{H^+,L^*} \Gamma_{\nu_f\mu}^{H^+} \right) \frac{m_b}{m_\mu} x(1-x) - \left( \Gamma_{tb}^{H^+,R^*} \Gamma_{\nu_f\mu}^{H^+} \right) \frac{m_t}{m_\mu} x(1+x) \right] \end{aligned} \quad (14)$$

where the loop function is defined as,

$$G(r^a, r^b) = \frac{\ln\left(\frac{r^a x + r^b(1-x)}{x(1-x)}\right)}{x(1-x) - r^a x - r^b(1-x)}, \quad (15)$$

and  $\Gamma_{tb}^{H^+,R}$  and  $\Gamma_{tb}^{H^+,L}$  are the couplings of  $H^+\bar{t}b$  if we write the vertex in the form of  $H^+\bar{t}(\Gamma_{tb}^{H^+,L} P_L + \Gamma_{tb}^{H^+,R} P_R)b$  with  $P_{R,L} = \frac{1}{2}(1 \pm \gamma^5)$ .

While for the  $\ell\nu_R$  loop when the heavy neutrinos enter into loop, the contribution can be obtained by replacing  $m_t$ ,  $m_b$ ,  $Q_t$  and  $Q_b$  by  $m_{\nu_R}$ ,  $m_\ell$ ,  $Q_\ell = -1$  and 0, respectively in Eq.(15).

#### IV. GLOBAL FIT OF THE 125 GEV HIGGS

We will perform a global fit to the 125 GeV Higgs signal data and a large number of observables. For the given neutral SM-like scalar-field  $h$  and its couplings, the  $\chi_h^2$  function

can be defined as

$$\chi_h^2 = \sum_k \frac{(\mu_k - \hat{\mu}_k)^2}{\sigma_k^2}, \quad (16)$$

where  $k$  runs over the different production(decay) channels considered, and  $\mu_k$  is the corresponding theoretical predictions for the MTH parameters.  $\hat{\mu}_k$  and  $\sigma_k$  denote the measured Higgs signal strengths and their one-sigma errors, respectively, and their choices in this work appear in [54], though the data and the references listed are not complete.

The Higgs signal strengths, employed in the experimental data on Higgs searches, measure the observable cross sections compared to the corresponding SM predictions. At the LHC, the SM-like Higgs particle is generated by the following production procedures: gluon fusion ( $gg \rightarrow H$ ), vector boson fusion ( $qq' \rightarrow qq'VV \rightarrow qq'H$ ), associated production with a vector boson ( $q\bar{q}' \rightarrow WH/ZH$ ), and the associated production with a  $t\bar{t}$  pair ( $q\bar{q}/gg \rightarrow t\bar{t}H$ ). Meanwhile, the Higgs decay channels are  $\gamma\gamma$ ,  $ZZ^{(*)}$ ,  $WW^{(*)}$ ,  $b\bar{b}$  and  $\tau^+\tau^-$ . The expressions of the Higgs signal strengths have been shown in [10] and we will not repeat here.

## V. CALCULATING RESULTS AND THE DISCUSSIONS

In Fig.2, we give the comparison of the contribution between the inner lines of the SM charged gauge bosons and the MTH heavy charged boson and that from the right-handed neutrino loop with the SM charged leptons. The green shadow area in the figure shows the discrepancy between the SM and the measurement for the anomalous magnetic moment  $\Delta a_\mu$ . From Fig.2 we can see the heavy mass of the gauge boson suppressing the contribution, and the contribution is smaller than that of the SM gauge boson, which can be seen in the lower two curves. And from the area of the discrepancy of the SM and the experiments, we can see that not only the heavy  $W_H^\pm$ , but also the SM  $W^\pm$ , both contribute much smaller the requirement with the heavy quark loop. So in the following, we will not consider the heavy gauge  $W_H^\pm$  and the quark loop. Instead, we consider the lepton  $\ell\nu_R$  loop contribution with the charged Higgs and the SM  $W^\pm$ , which is the top curve in Fig.2. From Fig.2 we can see that the contribution of the lepton loop is a little higher than the shadowed area, the parameters except the charged Higgs mass, however, are fixed. So we will scan them and pick up the optimum space ranges.

Fig.3 shows  $\Delta a_\mu$  varying with heavy neutrino mass and the coupling  $y_{\nu\ell}$ , from which we

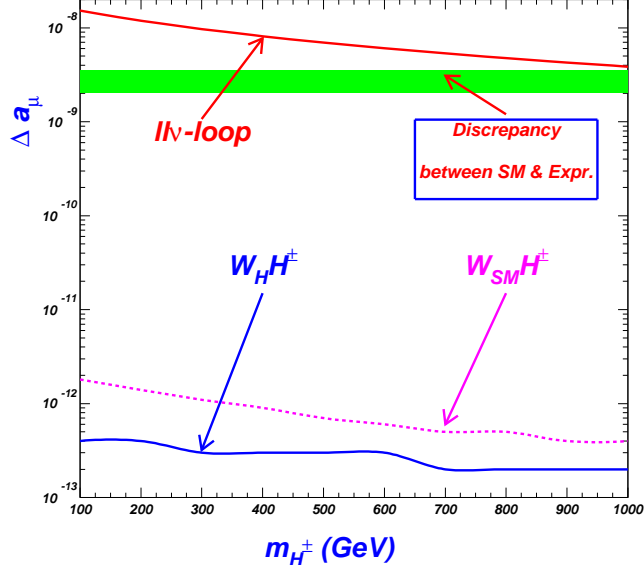


FIG. 2: The comparison between the inner lines of the SM charged gauge bosons and the MTH heavy charged boson (the below two curves). The contribution from the right-handed neutrino loop with the SM charged leptons are also considered (the above curve). The green shadow area is the discrepancy between the SM and the measurement for the anomalous magnetic moment  $\Delta a_\mu$ .

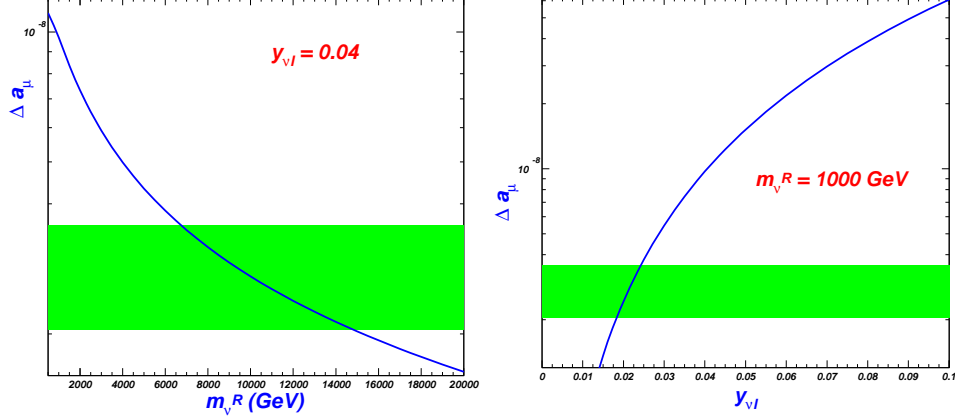


FIG. 3:  $\Delta a_\mu$  from  $ll\nu_R$  loop with the varying heavy neutrino mass (left) and the coupling  $y_{\nu l}$  (right).

can see the  $ll\nu_R$  loop can arrive at the requirement area.

In the following, we will scan the anomalous magnetic moment and the Higgs global fit by taking one million random points, so the more the points are left, the higher the possibility of the event is to be probed in the experiments. We restate the parameter ranges:  $100 \leq m_{H^\pm} \leq 1000$  GeV,  $500 \leq m_{\nu^R} \leq 20000$  GeV, and  $y_t, y_{\nu W} \sim 0 - 1.5$  times the values in SM, and  $y_{\nu l H^\pm} \leq 0.1$ .

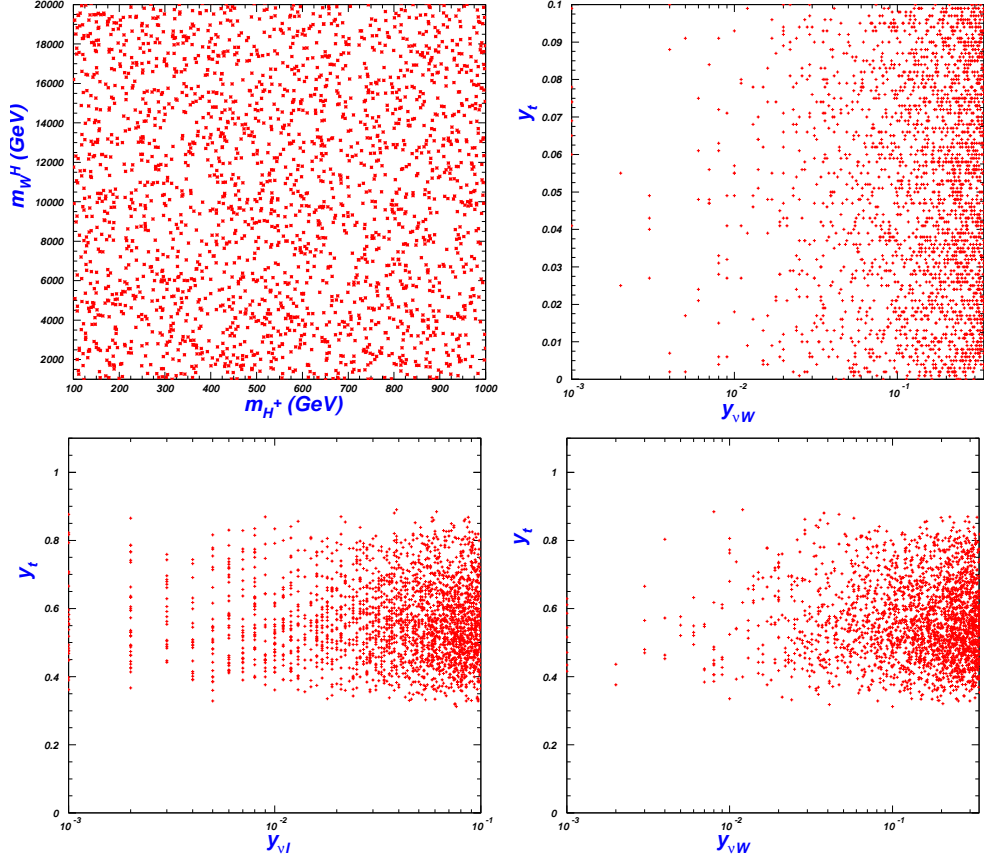


FIG. 4: The surviving samples within  $3\sigma$  ranges of  $\chi_h^2$  on the planes of  $m_{H^\pm} \sim m_{W^\pm}$ ,  $y_{\nu W} \sim y_t$ ,  $y_{\nu l} \sim y_t$  and  $y_{\nu W} \sim y_t$ .

In Fig. 4, we will show the surviving samples on the planes of  $m_{H^\pm} \sim m_{W^\pm}$ ,  $y_{\nu W} \sim y_t$ ,  $y_{\nu l} \sim y_t$  and  $y_{\nu W} \sim y_t$ , for the Higgs strengthen in the  $3\sigma$  confidence level. We find from the first diagram that the masses of the charged Higgs and the heavy gauge bosons are almost not constricted by the  $\chi_h^2$ , that is, they contribute little to the Higgs strengthen. Fig. 4 also shows that  $\chi_h^2$  favors larger couplings with the points concentrated in the top right-hand corner of the last three figures in Fig 4.

Note that we assume here the neutral Higgs in the MTH models does not mix with the charged Higgs, so there are only the heavy gauge boson mass and the top Yukawa coupling contributing to the  $\chi_h^2$  value. So in Fig. 4, we project the surviving samples within  $3\sigma$  range of  $\chi_h^2$  on the planes of  $y_t \sim m_{W^\pm}$ . We also consider the exclusion limits from the flavor changing constraints of  $\mu \rightarrow e\gamma$ [14]. Fig. 4 shows that  $\chi_h^2$  value favors a bit larger  $y_t$ , but almost no constraints to the charged gauge boson mass  $m_{W_H}$ , since the charged gauge boson only appear in the loop of the decay  $h \rightarrow \gamma\gamma$ , which is not dominant in the SM-like Higgs

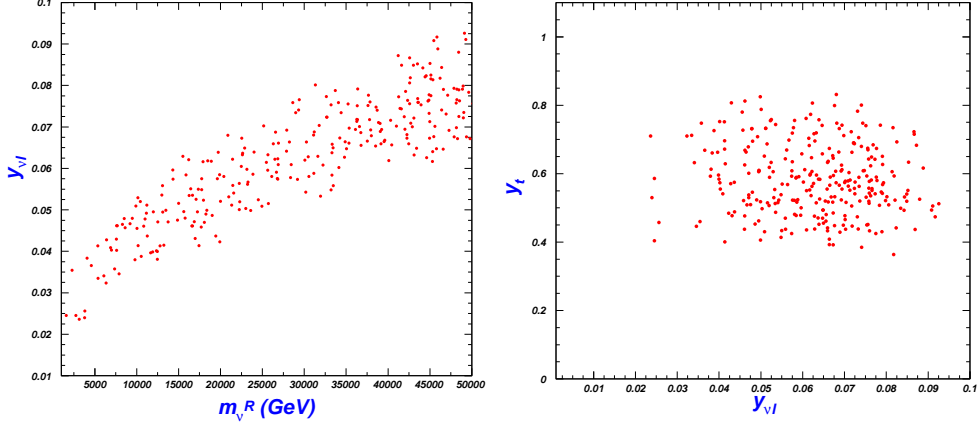


FIG. 5: The samples satisfying the constraints of Higgs global fit  $\chi_h^2$  within  $3\sigma$  range, on the planes of  $y_{\nu l H^\pm} \sim m_{\nu R}$  and  $y_{\nu l H^\pm} \sim y_t$ , with the constraints of the  $\Delta a_\mu$  from the experiments. All the samples are also constrained by muon decay  $\mu \rightarrow e\gamma$  and the precision electroweak data.

decay channels.

In Fig. 5, we project the surviving samples within  $3\sigma$  on the planes of  $m_{H^\pm} \sim m_{\nu R}$ ,  $y_{\nu l} \sim y_t$ ,  $y_{\nu l} \sim y_{\nu W}$  and  $y_{\nu W} \sim y_t$ , after imposing the associative constraints from the muon  $g-2$  anomaly and the Higgs global fit. From the first figure in Fig. 5, we can see the heavy neutrino mass contributes large, even when it is large. That is because, from Eq.(15) we can see that the  $g-2$  anomaly contribution is proportional to the heavy neutrino mass  $m_{\nu R}$ , when the function  $G$  in it is not considered.

We also see that from Eq.(15) that the  $g-2$  anomaly varies with  $y_{\nu l}^2$ , so coupling  $y_{\nu l}$  should matter much, which can be seen from the other figures in Fig. 5. This relevance will constrain  $y_{\nu l}$  greatly, and it can grossly read as  $0.03 \leq y_{\nu l} \leq 0.09$ . Another parameter which receive strong constraint is the top Yukawa coupling in MTH models, and from Eq.(15) we know if the quark loops contribute little and disregarded, the  $g-2$  anomaly is irrelevant with the parameter  $y_t$ . So the constraint comes mainly from the Higgs strengthen  $\chi_h^2$ . so we in the right figure of Fig. 5 give the allowed ranges of the twos with all the constraints, from which we can grossly get  $0.4 \leq y_t \leq 0.8$ .

Though we have scan all the parameters, the others such as  $m_{H^\pm}$ ,  $m_{W_H}$ ,  $y_{\nu W}$  are all not sensitive to the constraints, so we have not shown their ranges. As for the heavy neutrino mass  $m_{\nu R}$ , since, to  $\Delta a_\mu$ , it has the uplifting and suppressing effect at the same time, it is almost unlimited.

## VI. CONCLUSION

After imposing various relevant theoretical and experimental constraints, we performed a scan over the parameter space of this model to identify the ranges in favor of the muon  $g - 2$  explanation. We find that the muon  $g - 2$  anomaly can be explained in the MTH model in some parameter spaces. The Higgs direct search limits from LHC contribute most largely in all the constraints,. After imposing the joint constraints from the 125 GeV Higgs signal data, the precision electroweak data, and the leptonic decay, of all the parameters, we find that the muon  $g-2$  anomaly is sensitive to two parameters  $y_{\nu l}$ ,  $y_t$  with  $0.03 \leq y_{\nu l} \leq 0.09$  and  $0.4 \leq y_t \leq 0.8$ .

### Acknowledgment

This work was supported by the National Natural Science Foundation of China under grant 12075213, by the Fundamental Research Cultivation Fund for Young Teachers of Zhengzhou University(JC202041040) and the Academic Improvement Project of Zhengzhou University.

- 
- [1] H. N. Brown et al. [Muon  $g-2$  Collaboration], Phys. Rev. Lett. **86**, (2001) 2227, arXiv: hep-ex/0102017.
  - [2] C. Patrignani et al. (Particle Data Group), Chin. Phys. C40, 100001 (2016).
  - [3] G. W. Bennett et al. [Muon  $g-2$  Collaboration], Phys. Rev. D **73**, (2006) 072003, arXiv: hep-ex/0602035.
  - [4] T. Aoyama et al., arXiv:2006.04822.
  - [5] J. P. Miller, E. de Rafael, and B. L. Roberts, Rept. Prog. Phys. 70, 795 (2007), arXiv: hep-ph/0703049.
  - [6] F. Jegerlehner and A. Nyffeler, Phys. Rept. 477, 1 (2009), arXiv:0902.3360.
  - [7] J. P. Miller, E. de Rafael, B. L. Roberts, and D. Stockinger, Ann. Rev. Nucl. Part. Sci. 62, 237 (2012).
  - [8] M. Lindner, M. Platscher, and F. S. Queiroz, Phys. Rept. 731, 1 (2018), arXiv:1610.06587.
  - [9] F. Jegerlehner, Springer Tracts Mod. Phys. 274, pp.1 (2017).

- [10] Guo-Li Liu, Qing-Guo Zeng, Eur. Phys. Jour. C **79**, 612 (2019), arXiv:1811.04777.
- [11] Z. Chacko, H.-S. Goh, and R. Harnik, Phys. Rev. Lett. 96, 231802 (2006), arXiv: hep-ph/0506256.
- [12] M. Low, A. Tesi, L. Wang, Phys. Rev. D **91**, 095012 (2015), arXiv:1501.07890.
- [13] J. Serra, S. Stelzl, R. Torre, A. Weiler, JHEP10(2019)060, arXiv:1905.02203.
- [14] Guo-Li Liu, Fei Wang, Wenyu Wang, arXiv:2012.09986.
- [15] Junjie Cao, Peihua Wan, Lei Wu, Jin Min Yang, Phys. Rev. D **80**, 071701, (2009), arXiv:0909.5148.
- [16] Junjie Cao, Jingwei Lian, Lei Meng, Yuanfang Yue, Pengxuan Zhu, Phys. Rev. D 101, 095009 (2020), arXiv:1912.10225.
- [17] P. Fayet, Phys. Lett. 69B, 489 (1977).
- [18] S. Dimopoulos and H. Georgi, Nucl. Phys. B193, 150 (1981).
- [19] N. Arkani-Hamed, A. G. Cohen, and H. Georgi, Phys. Lett. B513, 232 (2001), arXiv: hep-ph/0105239.
- [20] H. Murayama, "supersymmetry phenomenology" in "proceedings, Summer School in Particle Physics: Trieste, Italy, June 21-July 9, 1999" pp. 296-335. 2000, arXiv: hep-ph/0002232.
- [21] L. Maiani, Conf. Proc.C7909031,1(1979);
- [22] D. B. Kaplan and H. Georgi, "SU(2) x U(1) Breaking by Vacuum Misalignment", Phys. Lett. 136B (1984) 183-186, D. B. Kaplan, H. Georgi, and S. Dimopoulos, "Composite Higgs Scalars", Phys. Lett. 136B (1984) 187-190.
- [23] S. Weinberg, Phys. Rev. D13, (1976) 974; *ibid*, D19, (1979) 1277; L. Susskind, Phys. Rev. D20, (1979) 2619; E. Farhi, L. Susskind, Phys.Rept.74, (1981) 277, C. T. Hill, Phys. Lett. B **345**, 483 (1995), arXiv: hep-ph9411426; K. Lane and E. Eichten, Phys. Lett. B **352**, 383 (1995), arXiv: hep-ph/9503433; K. Lane, Phys. Lett. B **483**, 96 (1998), arXiv: hep-ph/9805254; G. Cvetič, Rev. Mod. Phys.71, 513 (1999), arXiv: hep-ph/9702381; C. T. Hill and E. H. Simmons, Phys. Rept.**381**, (2003) 235-402; Erratum-*ibid*.390, (2004) 553, arXiv: hep-ph/0203079.
- [24] ATLAS Collaboration, M. Aaboud et al., Phys. Rev. D98 (2018), 032008, arXiv:1803.10178; CMS Collaboration, A. M. Sirunyan et al., JHEP 05 (2018) 025, arXiv:1802.02110; ATLAS Collaboration, G. Aad et al., Phys. Lett. B758 (2016) 249-268, arXiv:1602.06034; CMS Collaboration, A. M. Sirunyan et al., JHEP 08 (2018) 177, arXiv:1805.04758.
- [25] A Predictive Mirror Twin Higgs with Small Z2 Breaking Keisuke Harigaya, Robert McGehee,

- Hitoshi Murayama, Katelin Schutz, JHEP **05(2020)155**, arXiv:1905.08798.
- [26] R. Barbieri, T. Gregoire, and L. J. Hall, (2005), arXiv: hep-ph/0509242.
- [27] Z. Chacko, Y. Nomura, M. Papucci, and G. Perez, JHEP 01, 126 (2006), arXiv: hep-ph/0510273.
- [28] G. Burdman, Z. Chacko, H.-S. Goh, and R. Harnik, JHEP 02, 009 (2007), arXiv: hep-ph/0609152.
- [29] H. Cai, H.-C. Cheng, and J. Terning, JHEP 05, 045 (2009), arXiv:0812.0843.
- [30] D. Poland and J. Thaler, JHEP 11, 083 (2008), arXiv:0808.1290.
- [31] B. Batell and M. McCullough, Phys. Rev. D92, 073018 (2015), arXiv:1504.04016.
- [32] J. Serra and R. Torre, Phys. Rev. D 97, (2018) 035017, arXiv:1709.05399.
- [33] Csaba Csáki, T. Ma, and J. Shu, Phys. Rev. Lett. 121, (2018) 231801, arXiv:1709.08636.
- [34] Zackaria Chacko, Can Kilic, Saereh Najjari, Christopher B. Verhaaren, Phys. Rev. D 97, 055031 (2018), arXiv:1711.05300.
- [35] J. C. Pati and A. Salam, Phys. Rev. D 10, 275 (1974); R. N. Mohapatra and J. C. Pati, Phys. Rev. D11, 566(1975); R. N. Mohapatra and J. C. Pati, Phys. Rev. D11, 2558 (1975).
- [36] R. Barbieri, D. Greco, R. Rattazzi, and A. Wulzer, The Composite Twin Higgs scenario, arXiv:1501.07803.
- [37] P. Batra and Z. Chacko, A Composite Twin Higgs Model, Phys.Rev. D79 (2009) 095012, arXiv:0811.0394.
- [38] W. Emam and S. Khalil, Eur. Phys. J. C **55**, 625 (2007), arXiv:0704.1395.
- [39] W. Abdallah, A. Awad, S. Khalil, H. Okada, Eur. Phys. J. C 72(2012)2108, arXiv:1105.1047.
- [40] Z. Maki, M. Nakagawa and S. Sakata, Prog. Theor. Phys. **28**, 870 (1962).
- [41] A.G. Akeroyd (Taiwan, Natl. Cheng Kung U.), Mayumi Aoki (Tokyo U., ICRR), Hiroaki Sugiyama, Phys.Rev.D77:075010,2008, arXiv:0712.4019.
- [42] Hock-Seng Goh, Shufang Su, Phys. Rev. D **75**, (2007)075010, arXiv: hep-ph/0611015.
- [43] MEG Collaboration, J. Adam et al., Phys. Rev. Lett. **110**, (2013) 201801, arXiv:1303.0754; MEG Collaboration, A. M. Baldini et al., Eur. Phys. Jour. C **76 (2016)**, no. 8 434, arXiv:1605.05081.
- [44] G. Aad et al. [ATLAS Collaboration], arXiv:1903.06248.
- [45] CMS Collaboration [CMS Collaboration], Search for a narrow resonance in high-mass dilepton final states in proton-proton collisions using 140 fb<sup>-1</sup> of data at  $\sqrt{s} = 13$  TeV, CMS-PAS-EXO-

19-019.

- [46] G. Aad et al. [ATLAS Collaboration], Phys. Rev. D **100**, 052013 (2019), arXiv:1906.05609.
- [47] M. Tanabashi et al. [Particle Data Group], Review of Particle Physics, Phys. Rev. D **98**, no. 3, 030001 (2018). doi:10.1103/PhysRevD.98.030001.
- [48] G. Altarelli, B. Mele and M. Ruiz-Altaba, Z. Phys. C **45**, 109 (1989) Erratum: [Z. Phys. C **47**, 676 (1990)]. doi:10.1007/BF01552335, 10.1007/BF01556677.
- [49] A. Pankov, P. Osland, I. Serenkova and V. Bednyakov, Eur. Phys. Jour. C **80**, 503 (2020), arXiv:1912.02106.
- [50] A. Broggio, E. J. Chun, M. Passera, K. M. Patel and S. K. Vempati, JHEP **1411** (2014) 058, arXiv:1409.3199; L. Wang and X. F. Han, JHEP **05**, 039 (2015), arXiv:1412.4874; A. Dedes and H. E. Haber, JHEP **0105 (2001) 006**, arXiv: hep-ph/0102297; J. F. Gunion, JHEP **0908**, (2009) 032, arXiv:0808.2509; K. M. Cheung, C. H. Chou and O. C. W. Kong, Phys. Rev. D **64**, (2001) 111301, arXiv: hep-ph/0103183; D. Chang, W. F. Chang, C. H. Chou and W. Y. Keung, Phys. Rev. D **63 (2001) 091301**, arXiv: hep-ph/0009292; M. Krawczyk, Acta Phys. Polon. B33, (2002) 2621, arXiv: hep-ph/0208076; F. Larios, G. Tavares-Velasco and C. P. Yuan, Phys. Rev. D **64**, (2001) 055004, arXiv: hep-ph/0103292; K. Cheung and O. C. W. Kong, Phys. Rev. D **68**, (2003) 053003, arXiv: hep-ph/0302111; A. Arhrib and S. Baek, Phys. Rev. D **65**, (2002) 075002, arXiv: hep-ph/0104225; S. Heinemeyer, D. Stockinger and G. Weiglein, Nucl. Phys. B **690**, (2004) 62, arXiv: hep-ph/0312264; O. C. W. Kong, arXiv: hep-ph/040201; K. Cheung, O. C. W. Kong and J. S. Lee, JHEP **0906**, (2009) 020, arXiv:0904.4352.
- [51] Victor Ilisie, JHEP **04**, (2015) 077, arXiv:1502.04199.
- [52] A. Crivellin, J. Heeck, P. Stoffer, Phys. Rev. Lett. **116**,(2016) 081801, arXiv:1507.07567.
- [53] Mariana Frank, Ipsita Saha, arXiv:2008.11909.
- [54] ATLAS Collaboration, Phys. Rev. D **98**, (2018) 052003, arXiv:1807.08639; CMS Collaboration, Phys. Lett. B **780**, (2018) 501, arXiv:1709.07497; CMS Collaboration, JHEP **03**, (2019) 026, arXiv:1804.03682.